Potential energy curves and spin-orbit coupling of light alkali-heavy rare gas molecules

E. Galbis, J. Douady, E. Jacquet, E. Giglio, and B. Gervais

Articles you may be interested in

Ab initio many-electron study for the low-lying states of the alkali hydride cations in the adiabatic representation
J. Chem. Phys. **136**, 124304 (2012); 10.1063/1.3695997

An accurate model potential for alkali neon systems
J. Chem. Phys. **131**, 214104 (2009); 10.1063/1.3269801

Dynamics of spin–orbit recoupling in collisions of alkali atoms with noble-gas atoms using atomic core potentials
J. Chem. Phys. **119**, 12316 (2003); 10.1063/1.1625917

The 4 3 Σ + state of NaK: Potential energy curve and hyperfine structure
J. Chem. Phys. **119**, 4743 (2003); 10.1063/1.1590638

Spectroscopy of ionic alkali rare gas excimers in matrices
J. Chem. Phys. **106**, 3920 (1997); 10.1063/1.473782

Potential energy curves and spin-orbit coupling of light alkali-heavy rare gas molecules

E. Galbis, J. Douady, E. Jacquet, E. Giglio, and B. Gervais[a)]
CIMAP, unité mixte CEA-CNRS-ENSICAEN-UCBN 6252 BP 5133, F-14070 Caen, Cedex 05, France

The potential energy curves of the X, A, and B states of alkali-rare gas diatomic molecules, MKr and MXe, are investigated for M = Li, Na, K. The molecular spin-orbit coefficients $a(R) = \langle ^2\Pi_{\frac{1}{2}} | \hat{H}_{SO} | ^2\Pi_{\frac{1}{2}} \rangle$ and $b(R) = \langle ^2\Pi_{-\frac{1}{2}} | \hat{H}_{SO} | ^2\Sigma_{\frac{1}{2}} \rangle$ are calculated as a function the interatomic distance R. We show that $a(R)$ increases and $b(R)$ decreases as R decreases. This effect becomes less and less important as the mass of the alkali increases. A comparison of the rovibrational properties deduced from our calculations with experimental measurements recorded for NaKr and NaXe shows the quality of the calculations. © *2013 American Institute of Physics*. [http://dx.doi.org/10.1063/1.4773019]

I. INTRODUCTION

The alkali (M)-rare gas (RG) dimers constitute a class of van der Waals molecules, whose electronic structure is conceptually simple. The lowest excited states of these molecules, located below the first excitation threshold of the RG, are mapped onto the alkali excited states and can be described as one single electron on top of two closed-shell cores. This relative simplicity is particularly convenient to investigate more complex situations when the M is coupled to additional rare gas atoms at the surface of RG clusters, or trapped in RG matrices, and to unravel the fine details of the guest-hosts interaction. Models based either on diatomics-in-molecules[1–3] or on core polarization potential (CPP)[4,5] have been used to investigate these more complex situations. In both cases, reliable potential energy curves (PEC) for dimers are necessary to parameterize or to assess the quality of the models.

The aim of this work is to provide reliable potential energy curves for the lowest states of MKr and MXe, for the lightest alkali (M = Li, Na, K) and to investigate the effect of spin-orbit (SO) coupling on the potential energy curves and the corresponding vibrational states. Previous studies of the ground and lowest excited states of alkali-RG dimers have been performed. Experimentally, very accurate rovibrational spectrum were recorded for LiHe,[6] LiNe,[7] LiAr,[8] NaNe,[9,10] NaAr,[11] NaKr,[12,13] NaXe,[14] and also KAr.[15] These measurements were used to extract potential energy curves for the $X^2\Sigma$ state and the excited $A^2\Pi_{\frac{1}{2}}$ and $A^2\Pi_{\frac{3}{2}}$ states. From a theoretical point of view, numerous model calculation based on CPP approach have been performed.[15,16,21–23] Correlated methods, either configuration interaction or coupled cluster, were used recently for molecules made of Li and light RG.[16,17]

Previous theoretical studies of Li-RG reported a large anomalous molecular spin-orbit effect.[18,19] This effect becomes more and more pronounced as the mass of the rare gas increases. There is unfortunately no experimental data available for LiKr or LiXe and a direct comparison with experimental data was thus not possible. In their experimental studies of Na-RG, Zimmermann and co-workers[11–14] observed a similar effect. However, the analysis of the experimental rovibrational spectrum for heavy rare gas is more difficult than for light rare gas because of the contribution of several isotopes with comparable abundance. For the highest vibrational levels, the density of vibrational states increases near the dissociation limit and the proximity of the free atom lines makes the experimental analysis quite difficult. Moreover, the $^2\Sigma^+$ and $^2\Pi$ states are coupled together by SO interaction. In the corresponding energy range, the assignment of the vibrational levels is thus delicate, making the extraction of potential energy curves difficult. A better knowledge of the spin-orbit coupling between these states is certainly helpful to analyze the data. Our work bridges the gap between experiment and theory by providing theoretical data and a detailed critical analysis of the NaKr and NaXe results.

For heavy alkali like Rb and Cs, the $A^2\Pi$ states are dominated by SO coupling, which can be larger than the spin-free binding energy. For light alkali subject to this paper, the spin-orbit interaction is much smaller than the spin-free interaction. The variation of the coupling with respect to interatomic distance R has been reported only for the $^2\Pi$ states of Li-RG dimers.[18,19] For a complete analysis, however, the coupling between $^2\Sigma^+$ and $^2\Pi$ states is necessary. A more systematic investigation for different alkali is thus desirable to analyze this aspect.

Our paper is organized as follows. Section II summarizes the method used to determine the electronic structure. The results for the $X^2\Sigma^+$ ground state of the dimers are presented in Sec. III. The results of the spin-orbit matrix elements are discussed in Sec. IV. We combine the calculation of adiabatic $A^2\Pi$ and $B^2\Sigma^+$ states with the spin-orbit coupling to investigate the vibrational properties of the dimers excited states, which are discussed in Sec. V. The accuracy of our calculation is estimated by comparison of the vibrational spectrum with available experimental results. Section VI gives our concluding remarks.

---

a)Author to whom correspondence should be addressed. Electronic mail: gervais@ganil.fr.

138, 014314-1

II. COMPUTATIONAL METHODS

Alkali-rare gas dimers are weakly bound systems dominated by dispersion interaction. It is thus necessary to use explicitly correlated methods to obtain reliable PECs. On one hand, couple cluster calculation including full single and double excitations and triple excitation as a perturbation (CCSD(T)) were carried out to examine the $X^2\Sigma^+$ and $A^2\Pi$ states of the MRG molecules using MOLCAS code.[20] On the other hand, complete active space with second order perturbation theory (CASPT2) calculations were performed to examine the $B^2\Sigma^+$ state of the MRG molecules. Both methods are size consistent, which is important when the number of correlated electrons increases. The computation of the $B^2\Sigma^+$ PEC was completed by model calculations similar to those used for Ne and Ar[5,21–23] and adapted for Kr.

Though not overwhelming, the relativistic effects are not completely negligible for atoms like Kr and Xe. They were taken into account by means of Douglas-Kroll-Hess correction.[24,25]

We performed an all-electron calculation. As a trade-off between computation time and accuracy, the inner-shell orbitals were kept frozen as follows. We denote by n the principal quantum number of the valence alkali orbital, and by m the principal quantum number of the outermost rare gas p orbital. For the alkali, the outer $(n-1)s$, $(n-1)p$ and ns orbitals were explicitly correlated in the CCSD(T) calculation. For the rare gas, the outer ms, mp and also $(m-1)d$ orbitals were explicitly correlated in the CCSD(T) calculation. The basis sets employed were full atomic natural orbitals with relativistic core contraction, contracted to get valence quadruple-zeta plus polarization quality,[26,27] and extended with at least one additional diffuse function for all alkali and rare gas. The innermost orbitals were kept contracted as in the original basis set, while the outermost orbitals were uncontracted as follows: $(15s, 10p, 6d, 4f, 2g, 1h)/[13s, 10p, 6d, 4f, 2g, 1h]$ for Li, $(18s, 13p, 7d, 5f, 3g, 2h)/[14s, 12p, 7d, 5f, 3g, 2h]$ for Na, $(23s, 18p, 8d, 6f, 4g, 3h)/[16s, 14p, 8d, 6f, 4g, 3h]$ for K, $(21s, 18p, 12d, 5f, 3g, 2h)/[14s, 12p, 9d, 5f, 3g, 2h]$ for Kr, and $(23s, 20p, 14d, 6f, 4g, 2h)/[15s, 13p, 11d, 6f, 4g, 2h]$ for Xe. The basis set superposition error (BSSE) has been corrected at each point of all potential energy curves using the counterpoise method.[28]

Using the above basis set and CCSD(T) method, the atomic $ns - np$ transition energies are 14 912.4 cm^{-1} for Li, 16 979.9 cm^{-1} for Na, and 13 012.8 cm^{-1} for K. They compare fairly well with the experimental values taken as the average of the two fine structure components: 14 903.9 cm^{-1} for Li, 16 967.6 cm^{-1} for Na, and 13 023.8 cm^{-1} for K.[29] A calculation of the ground state of the cationic counterparts, M^+RG, shows that these basis sets are somewhat comparable to those used by Viehland and co-workers.[31–33] The main differences between this series of calculations and ours are essentially the number of correlated electrons, and the use of an all-electrons scheme instead of pseudopotentials. Our calculations for M^+RG lead actually to slightly deeper potential wells and slightly shorter equilibrium distances.

Finally, we obtained the molecular spin-orbit splitting as a function of the intermolecular distance by combining the

two Π and the Σ states obtained by a restricted active space (RAS) self-consistent field (SCF) calculation with the above basis sets in the RAS state interaction approach provided in MOLCAS. In the basis set $|\Lambda, M_S\rangle$, $(|1, \frac{1}{2}\rangle; |1, -\frac{1}{2}\rangle; |0, \frac{1}{2}\rangle)$, where Λ and M_S are, respectively, the orbital momentum and spin projections onto the molecular axis, the potential energy matrix V including SO is given by

$$V = \begin{pmatrix} V_\Pi + a & & \\ & V_\Pi - a & b\sqrt{2} \\ & b\sqrt{2} & V_\Sigma \end{pmatrix}, \quad (1)$$

where

$$a(R) = \left\langle 1, \frac{1}{2} \right| \hat{H}_{SO} \left| 1, \frac{1}{2} \right\rangle, \quad (2)$$

$$b(R) = \left\langle 1, -\frac{1}{2} \right| \hat{H}_{SO} \left| 0, \frac{1}{2} \right\rangle, \quad (3)$$

and V_Π and V_Σ are the spin free potential energies.

III. THE $X^2\Sigma^+$ GROUND STATE

The potential wells of the $X^2\Sigma^+$ state of the MRG dimers are depicted in Figures 1 and 2. The corresponding computed values are given as the supplementary material.[34] The equilib-
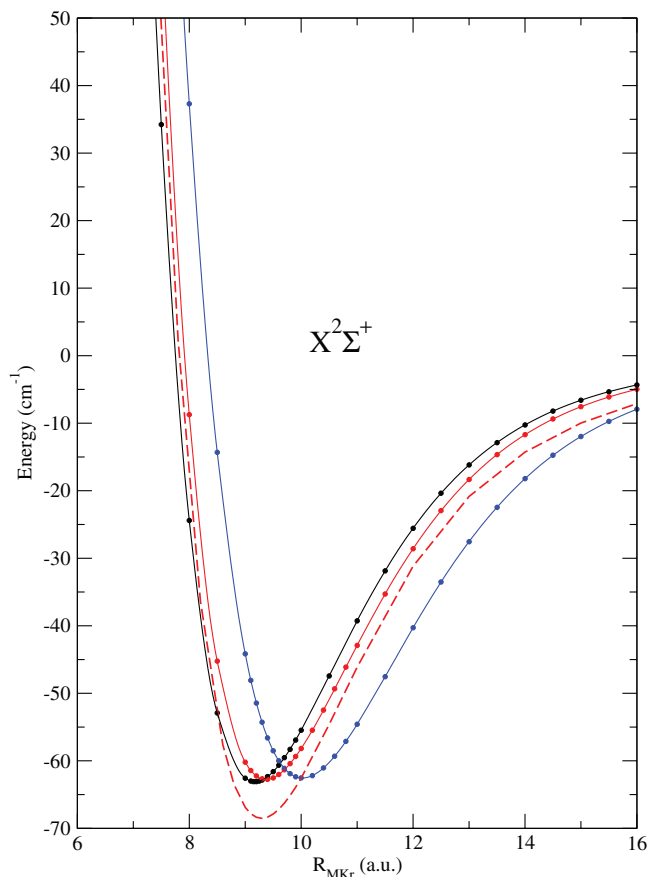

FIG. 1. Potential energy curves of the ground states $X^2\Sigma^+$ of MKr dimers (black: M = Li, red M = Na, blue M = K). Present CCSD(T) calculation: points interpolated by continuous lines. Experimental fitting for NaKr: dashed lines.[13]

FIG. 2. Potential energy curves of the ground states $X^2\Sigma^+$ of MXe dimers (black: M = Li, red M = Na, blue M = K). Present CCSD(T) calculation: points interpolated by continuous lines. Experimental fitting for NaXe: dashed lines.[14]
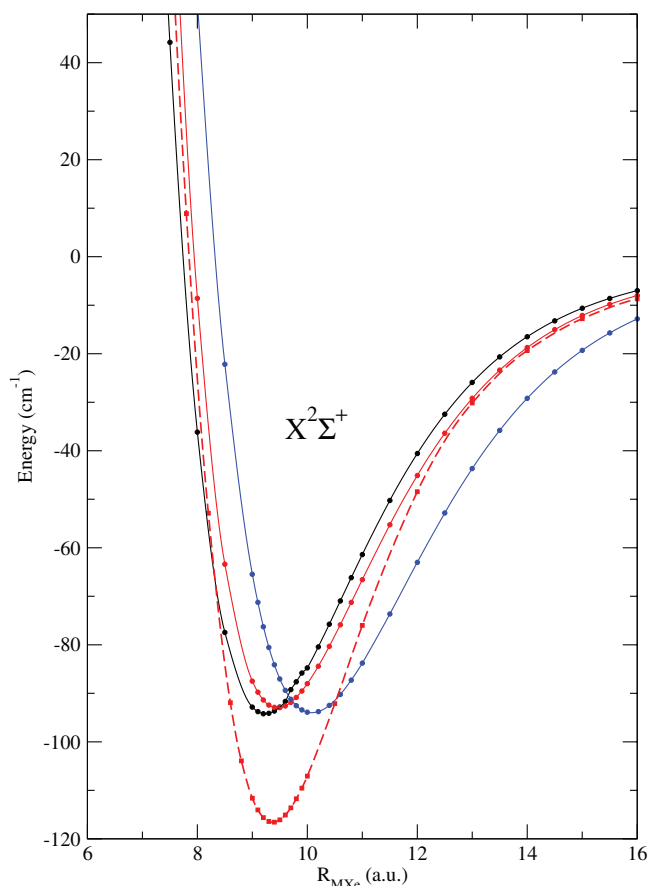
TABLE I. Experimental and theoretical bond length (in atomic units) and dissociation energies (in cm^{-1}) for the $X^2\Sigma^+$ state of MKr molecules. PW: present work.

Molecule	Reference	Method	R_e	D_e
LiKr	38	Expt.	9.20	69.0
	39	Expt.	8.79	63.9
	40	Expt.	9.03	68.0
	19	MRCI	9.20	59.0
	17	RCCSD(T)	9.26	60.0
	PW	CCSD(T)	9.16	63.1
NaKr	38	Expt.	9.37	69.0
	39	Expt.	8.94	69.0
	12	Expt.	9.30	69.0
	13	Expt.	9.30	68.4
	PW	CCSD(T)	9.39	62.8
KKr	38	Expt.	9.90	71.5
	39	Expt.	9.15	73.0
	39	Expt.	10.13	68.5
	PW	CCSD(T)	10.03	62.5

For NaKr, a comparison of our calculation with the fit extracted from experiment[13] is shown in Figure 1. The shape of the potential wells are different, in particular for interatomic distances $R > 12$ a.u. The long-range coefficient deduced from experiment ($C_6 = 1800$ a.u.[13]) is far above the most recent estimated value ($C_6 = 293$ a.u.[35]) and also larger than the upper bound determined by Standard and Certain ($C_6 = 737$ a.u.[36]). Nevertheless, the vibrational analysis of our computed PEC gives 10 vibrational bound states for a rotational number $L = 0$, just like the fit extracted from experimental values. The energy difference between the lowest vibrational levels are $\nu_{01} = 12.75$ cm^{-1} and $\nu_{02} = 23.90$ cm^{-1} to be compared with the corresponding experimental values $\nu_{01} = 13.19$ cm^{-1} and $\nu_{02} = 24.75$ cm^{-1}. The difference corresponds to a few rotational levels only, meaning that the calculated PEC is consistent with the experimental results. The analysis with respect to the basis set size shows that a systematic increase by 1 more diffuse orbital for each angular momentum deepens the potential well by 1 cm^{-1} and reduces the C_6 coefficient, producing thus a narrower well and larger

rium distances R_e and well depths D_e are summarized in Tables I and II. For a given alkali, R_e is only slightly smaller for Kr than for Xe. On the contrary, the well depth changes from Kr to Xe by a factor comparable to the ratio of the rare gas polarizabilities. Generally speaking, the comparison of our calculated D_e with experimental data suggests that the calculated potential wells should be slightly deeper, by roughly 10%. The difference may come from correlation effect not included in the CCSD(T) calculation. Indeed, when looking at D_e for the series of dimers investigated here, the difference between the CCSD and CCSD(T) calculations ranges from 25% for LiKr to 35% for KXe, which indicates that a high level of electronic correlation is important to obtain reliable data.

For LiKr dimer, our calculation gives a potential well slightly deeper and shorter than the theoretical results of Kerkines and Mavridis.[17] The main differences between both calculation are the relativistic effects and the d shell correlation. Both features contribute to the contraction of the electronic cloud, which leads to a shorter bond length. The relativistic multi-references configuration interaction (MRCI) calculation of Park *et al.*[19] is relatively close to the CCSD(T) results, but it seems that the BSSE was not removed, so that this result is only a lower estimate. The comparison of our results with this MRCI calculation for LiXe leads to similar conclusions.

TABLE II. Experimental and theoretical bond length (in atomic units) and dissociation energies (in cm^{-1}) for the $X^2\Sigma^+$ state of MXe molecules. PW: present work.

Molecule	Reference	Method	R_e	D_e
LiXe	38	Expt.	9.26	106.2
	40	Expt.	9.07	102.3
	19	MRCI	9.28	96.0
	PW	CCSD(T)	9.25	94.2
NaXe	38	Expt.	9.56	104.7
	39	Expt.	9.28	100.2
	14	Expt.	9.37	116.6
	PW	CCSD(T)	9.48	93.0
KXe	38	Expt.	9.92	110.7
	39	Expt.	9.82	102.7
	PW	CCSD(T)	10.08	94.0

vibrational level spacing. Besides the residual basis set effect and the molecular effects beyond the Born-Oppenheimer approximation, which are likely to be small, the dynamical correlation will definitely produce a narrower potential well without necessarily making it deeper.

Considering the repulsive part of the NaKr ground state PEC, our calculation is in global agreement with the experimental fit[13] as it can be observed in Figure 1. Our CCSD(T) PEC is slightly above the fitted curve by 50–10 cm^{-1} for R ranging between 5.5 and 7.5 a.u., i.e., in the energy range 0–1400 cm^{-1}. Regarding the intrinsic limitation of the calculation and of the extraction procedure from experimental data, this agreement should be considered as excellent.

The NaXe dimer has been also investigated by means of rovibrational spectroscopy.[14] The complexity of the analysis due to the large number of Xe isotopes allows to obtain only the lowest vibrational level for the $X\Sigma^+$ state. The long-range tail of the extracted PEC should therefore be considered as approximate. The experimentally fitted coefficient $C_6 = 664$ a.u. is within the boundaries given by Standard and Certain,[36] but 50% higher than the estimate from Mitroy and Zhang.[35] Our calculation is apparently a bit less accurate for Xe than for Kr. For ^{129}Xe our calculation gives 12 vibrational levels and a rotational constant $B_0 = 3.38 \times 10^{-2}$ cm^{-1}, instead of 13 levels and $B_0 = 3.47 \times 10^{-2}$ cm^{-1} from the experimental fit. Such a difference is partially accounted for by the small difference of 1% between calculated and experimental equilibrium distances. The relatively large difference between our calculation of D_e and the experimental value obtained by Baumann *et al.*[14] is more puzzling. There is no reason for our calculation to be significantly less accurate for Xe than for Kr. Assuming 10% underestimation of the well depth would lead to $D_e = 102$ cm^{-1}, in agreement with collisional experiments,[38,39] but at the lower limit deduced by Baumann *et al.*[14]

In the repulsive part of the NaXe ground state PEC, the shape of the calculated and experimental PEC are in close agreement. Our calculation overestimates the experimental values by 100 cm^{-1} typically. However, it must be noted that in this range, where the ground state PEC varies quickly with R, the quality of the potential extracted from fluorescence dispersion experiment depends on the shape of the upper $\Pi_{\frac{3}{2}}$ state,[14] and a small error on the upper PEC may lead to a more significant error on the ground state PEC.

There is much less data for KKr and KXe dimers. The K atom is significantly bigger than Li and Na, and larger equilibrium distances R_e are found. For both rare gas, Kr and Xe, the well depth of KRG is comparable to those of LiRG and NaRG, despite the larger polarizability of K. The comparison with experimental results from collision experiments suggests slightly deeper potential wells, like for the other alkali, as it can be observed in Tables I and II.

The long-range part of the PEC can be characterized by the leading dispersion coefficient C_n of the R^{-n} asymptotic expansion, with $n = 6, 8, 10$, and many calculations of these coefficients exist in the literature.[35,36] It is not easy to extract such a value from a fit to our calculated data. We define instead $Q(R) = R^6 V(R) \approx C_6 + C_8/R^2 + C_{10}/R^4 + \ldots$, where V(R) is the binding energy of the dimer. The

TABLE III. Asymptotic values of $Q(R) = R^6 V(R)$ and $Q^*(R) = C_6 + C_8/R^2 + C_{10}/R^4$ for MRG pairs at $R = 20$ a.u., for the $X^2\Sigma^+$ state. The coefficients C_n are taken from Ref. 35. All values are given in atomic units.

Dimer	$Q(20)$	$Q^*(20)$	C_6	$\frac{C_8}{R^2} + \frac{C_{10}}{R^4}$
LiKr	300	304	260	44
LiXe	480	486	411	75
NaKr	343	346	293	53
NaXe	550	552	461	91
KKr	607	551	444	107
KXe	980	878	698	180

values $Q(20)$ are compared to the results of the expansion obtained with the coefficient determined by Mitroy and Zhang[35] in Table III. The agreement is excellent for Li and Na. In the case of K, the values deduced from the expansion coefficients underestimate our calculations by 10% approximately, for both Kr and Xe. This difference might be accounted for by higher order coefficients C_n neglected in such a simple analysis.

The consistency between the estimated coefficients and our *ab initio* calculations suggests to constrain the asymptotic expansion of the potential when extracting a PEC from spectroscopic data, rather than fitting it, when the measured rovibrational states are concentrated around the equilibrium distance R_e, as it is usually the case.

IV. SPIN-ORBIT COUPLING

Before analyzing the excited PEC, it is necessary to investigate the spin-orbit coupling between the molecular states correlating asymptotically to the degenerate ^{2}P(np) states of the alkali. Inside this manifold, the spin-orbit is governed by the two values $a(R)$ and $b(R)$ defined in Sec. II. The $\Pi - \Pi$ coupling coefficient $a(R)$ has been the subject of previous investigation for Li,[18,19] but $b(R)$ was never studied, though it controls the shape of the PEC beyond $R = 10$ a.u. typically, for $\Omega = \frac{1}{2}$, where Ω is the projection of the total angular momentum onto the molecular axis. It was shown that the correlation has a minor effect on the variation of a with the interatomic distance R.

Our investigation is thus limited to the RASSCF calculation outlined in Sec. II. Beside this approximation, we used an atomic mean field integral (AMFI) approximation to evaluate the SO matrix elements.[30] The method is hereafter referred to as RASSCF-AMFI.

Such an approximation is not very accurate for bare alkali, and the asymptotic values were constrained to match the corresponding experimental values, simply by subtracting the computed atomic values and adding their experimental counterparts.[29]

The coefficients $a(R)$ and $b(R)$ are depicted in Figures 3 and 4. The computed values are given as the supplementary material.[34] Starting from the asymptotic value, $a(R)$ increases monotonically as R decreases, except at very short distance for potassium, where the overlap with the K$^+$ core becomes important. For LiKr and LiXe, our RASSCF-AMFI calculation agrees nicely with more elaborated rela-
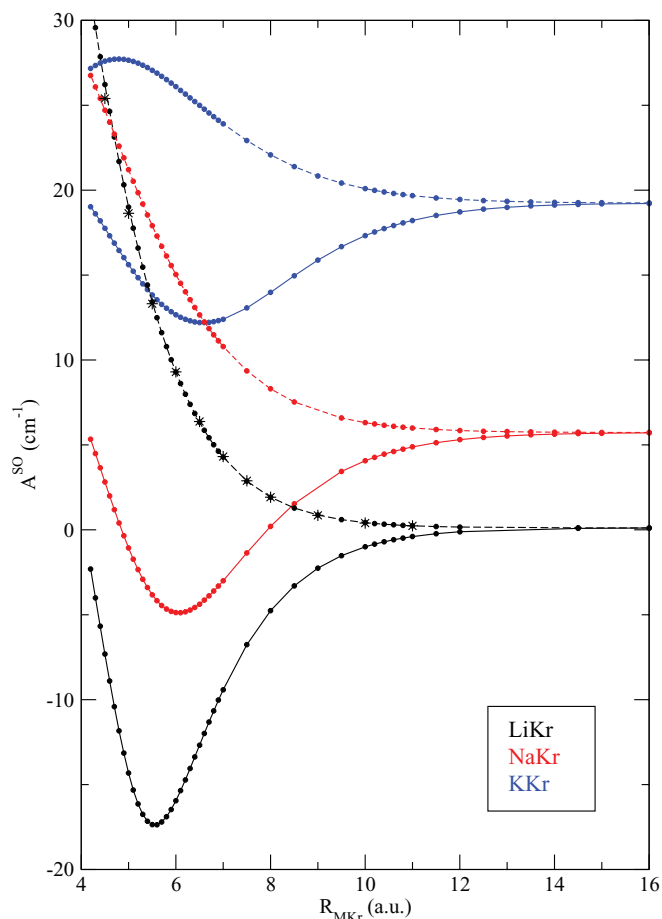
FIG. 3. Spin-orbit coupling for MKr dimers $a(R)$ and $b(R)$ (black: M = Li, red M = Na, blue M = K). The asymptotic value is set to the corresponding atomic value. Present RASSCF-AMFI calculation: $a(R)$ points interpolated by dashed lines; $b(R)$ points interpolated by continuous lines. MRCI results for LiKr: asterisks.[19]

FIG. 4. Spin-orbit coupling for MXe dimers $a(R)$ and $b(R)$ (black: M = Li, red M = Na, blue M = K). The asymptotic value is set to the corresponding atomic value. Present RASSCF-AMFI calculation: $a(R)$ points interpolated by dashed lines; $b(R)$ points interpolated by continuous lines. MRCI results for LiXe: asterisks.[19]

tivistic calculations.[19] The variations of $b(R)$ are significantly different from those of $a(R)$. Indeed, $b(R)$ decreases, possibly changes of sign to become negative, reaches a minimum and then increases as R decreases. Such a variation with the distance is comparable to the variation observed for the $(1^4\Pi, C^2\Delta)$ SO coupling of the BAr molecule.[37]

The R dependence of both coefficients reflects the differential occupation of the outer RG p shell with spin-up (α) and spin-down (β) electrons. In the quadrupole field of the excited ^2P state of the alkali atom, the RG atom is polarized. This polarization is characterized by a static dipole $d(R)$ with a magnitude varying up to 2 a.u. and oriented from the alkali to the rare gas at large distances. For Π state, $d(R)$ increases monotonically as R decreases, while its behavior for Σ state is more complex. For Li and Na, $d(R)$ vanishes approximately at the distance where the coefficient $b(R)$ is minimum and then change of sign. This behavior is not observed for K, for which only a shallow minimum is observed. The variation of $d(R)$ is associated with the reorganization of the valence electronic density. When the overlap between the valence orbital and the RG p orbitals becomes important for the Σ state, a part of the valence electronic density is pushed out of the rare gas core in the direction opposite to the alkali atom, changing eventually the orientation of the dipole.
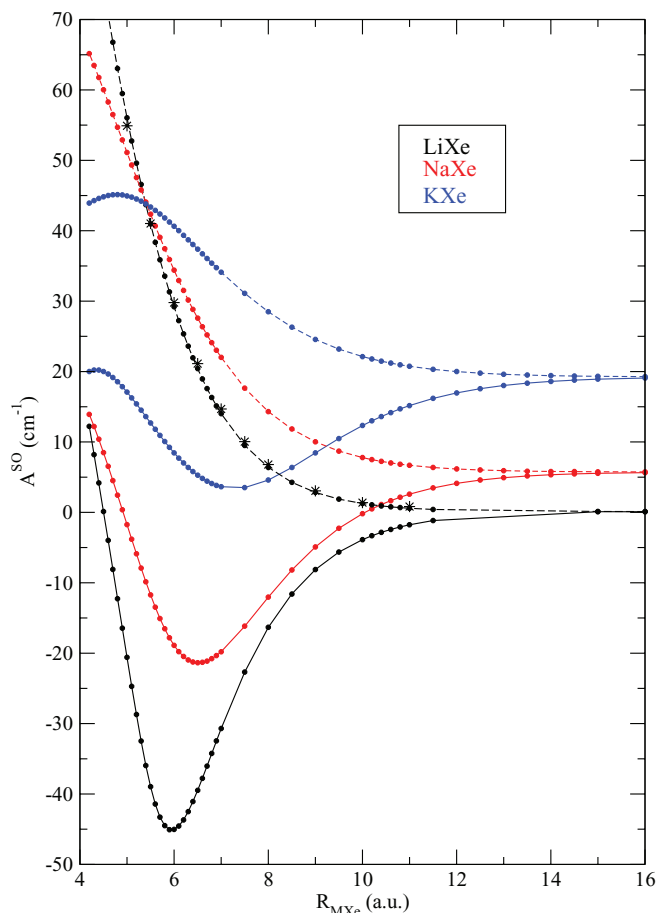
In a RASSCF-AMFI calculation like ours, the core orbitals are all doubly occupied with the same amount of α and β electrons. The rare gas polarization alone has thus no effect regarding the molecular SO effect. However, the valence p orbital gets hybridized with RG outer p shell to form an antibonding orbital with a definite spin orientation, α, for example. The hybridization is illustrated in Figure 5 for the $A^2\Pi$ state at an interatomic distance $R = 7$ a.u. The small RG p component acquired by the alkali valence orbital changes the net population of the α RG p orbital, giving an additional contribution to SO from the rare gas. For Π states, the antibonding hybridization is characterized by a $-$ sign, i.e., the valence orbital can be written as

$$|v_\Pi, \alpha\rangle = c_M |\pi_M, \alpha\rangle - c_{RG}|\pi_{RG}, \alpha\rangle, \qquad (4)$$

where c_M and c_{RG} have the same phase.

On the contrary for Σ states, the antibonding hybridization is characterized by a $+$ sign, i.e., the valence orbital can be written as

$$|v_\Sigma, \alpha\rangle = d_M |\sigma_M, \alpha\rangle + d_{RG}|\sigma_{RG}, \alpha\rangle, \qquad (5)$$

where d_M and d_{RG} have the same phase.

Using the above expressions together with the assumption of an atomic SO hamiltonian and a negligible overlap
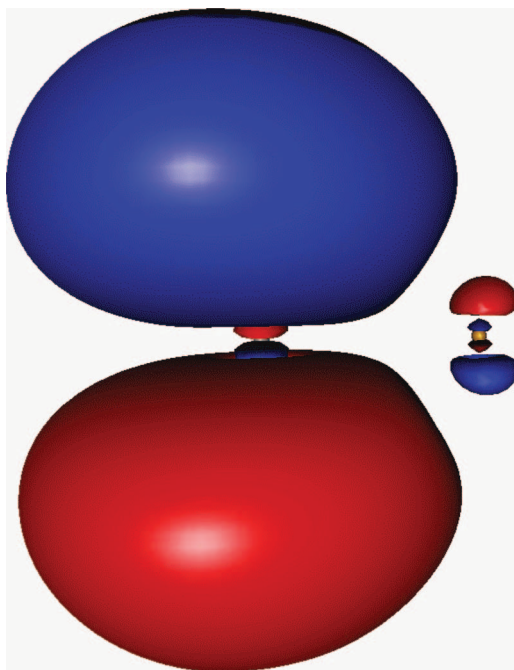
FIG. 5. Hybridization of the valence orbital of the NaKr molecule at a distance $R = 7$ a.u., for the $A^2\Pi$ state.

FIG. 6. Potential energy curves of the lowest excited states $A^2\Pi$ and $B^2\Sigma^+$ of MKr dimers (black: M = Li, red M = Na, blue M = K). Present CCSD(T) calculation: points interpolated by continuous lines. Experimental fitting for NaKr: long dashed line.[13] Present CASPT2 calculation: square interpolated by continuous lines. LiKr $B^2\Sigma^+$ from RCCSD(T): short dashed line.[17] NaKr $B^2\Sigma^+$ from experiment: stars.[43]

between M and RG orbitals, we obtained that the SO diagonal matrix element $a(R) = \langle v_\Pi, \alpha | \hat{H}_{SO} | v_\Pi, \alpha \rangle$ increases, while the off-diagonal element $b(R) = \langle v_\Pi, \beta | \hat{H}_{SO} | v_\Sigma, \alpha \rangle$ decreases. Note that the bonding or antibonding character is not essential, provided that v_Π and v_Σ have an opposite bonding character. It is also important to note that a simple orthogonalization of the alkali valence orbital to the rare gas core cannot explain the observed effect. In such a case indeed, the orthogonality implies that the projection onto the RG outer p shell SO operator vanishes by construction, so that no additional SO coupling is obtained. The present hybridization is more similar to a back donation effect, where the valence electron can occupy the RG outer p orbital liberated by polarization.

As expected from the above analysis, the variation of the SO coupling with the interatomic distance R is stronger for Xe than for Kr. For a similar hybridization in Kr and Xe systems, we expect a magnification of the effect by a factor 2. The effect is actually slightly more pronounced in Xe for which $a(R)$ is 3 times larger than for Kr in the vicinity of equilibrium positions. Regarding $b(R)$, it is interesting to note that it vanishes for LiKr and LiXe around $R = 11$ a.u. This distance coincides approximately to the $\Sigma - \Pi$ PEC crossing, where the weakness of the SO coupling is going to influence the vibrational spectrum of the corresponding molecules.

As we can see in both Figures 3 and 4, the lighter the alkali, the larger the variation of $a(R)$ and $b(R)$. This observation is consistent with the series of experiments performed on MAr,[8,15] which shows a clear decrease of the SO molecular effect as the mass of the alkali increases. We interpret this effect as another manifestation of the hybridization. Generally speaking, hybridization is more pronounced for two orbitals with comparable energies. The latter are of course quite dif-
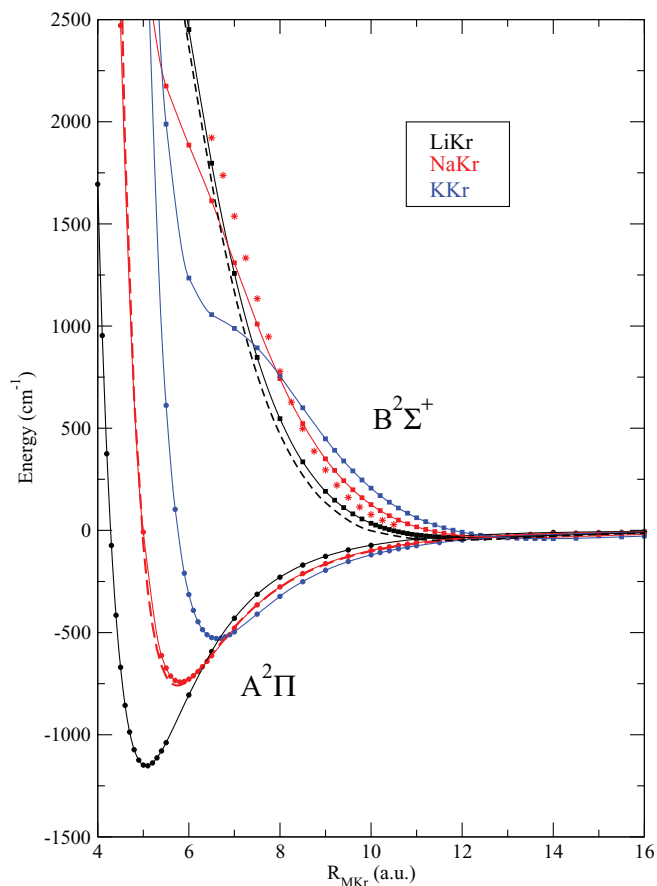
ferent for alkali and rare gas, but they are closer for Li than for Na and than for K.

V. EXCITED STATES

The SO free adiabatic PEC of the MKr and MXe excited states are presented in Figures 6 and 7, respectively. A summary of minimum positions R_e and corresponding well depth D_e for the $A^2\Pi$ states is given in Table IV for MKr and in Table V for MXe, where they are compared with some values collected from the literature. The computed values are given as the supplementary material.[34] The general trend is to produce larger D_e and R_e for Xe than for Kr, as expected from the respective polarizability and size of these two atoms. For the $A^2\Pi$ PEC, D_e and R_e increase as the atomic number of the alkali increases, following the size of the corresponding cationic core.

For the $B^2\Sigma^+$ PEC, the variation among the alkali is much less pronounced. Indeed, for a given RG, whatever the kind of calculation, either CASPT2 or model, the well depth of the $B^2\Sigma^+$ state is comparable for LiRG and NaRG and slightly larger for KRG. Regarding R_e, the Li atomic $2p$ orbital is less diffuse than the corresponding Na $3p$ and K $4p$
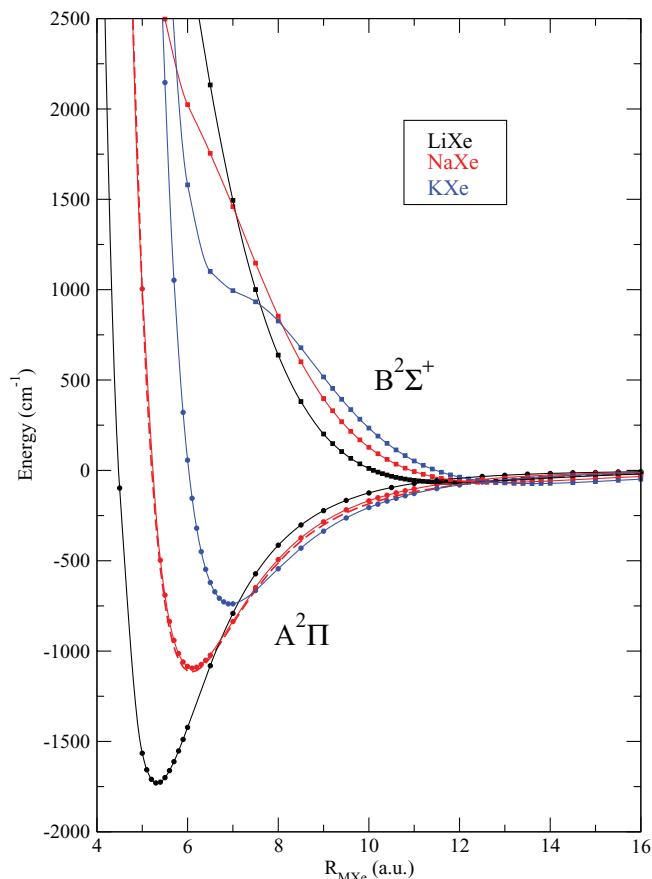
FIG. 7. Potential energy curves of the lowest excited states $A^2\Pi$ and $B^2\Sigma^+$ of MXe dimers (black: M = Li, red M = Na, blue M = K). Present CCSD(T) calculation: dot interpolated by continuous lines. Experimental fitting for NaXe: dashed lines.[14] Present CASPT2 calculation: square interpolated by continuous lines.

orbitals, so that R_e is shorter for LiRG than for NaRG and KRG. A summary of these values, which are less accurate for the B $^2\Sigma^+$ state than for the A $^2\Pi$ and X $^2\Sigma^+$ states, can be found in the supplementary material.[34]

Some *ab initio* calculations have been performed for LiKr.[17,19] For the $A^2\Pi$ state, our results are close to those obtained by Kerkines and Mavridis[17] with a comparable CCSD(T) method. The contraction observed for the ground

TABLE IV. Experimental and theoretical data on the $A^2\Pi$ state of MKr molecules. Methods, bond length (in atomic units), and dissociation energies (in cm^{-1}). PW: present work.

Molecule	Reference	Method	R_e	D_e
LiKr	41	Expt.	6.18	1200
	19	MRCI ($A^2\Pi_{1/2}$)	5.16	917
	19	MRCI ($A^2\Pi_{3/2}$)	5.20	867
	17	RCCSD(T)	5.05	1220
	PW	CCSD(T)	5.06	1159
NaKr	42	Expt.	6.14	730
	13	Expt. ($A^2\Pi_{1/2}$)	5.73	795
	13	Expt. ($A^2\Pi_{3/2}$)	5.76	760
	PW	CCSD(T)	5.80	742
KKr	PW	CCSD(T)	6.62	530

TABLE V. Experimental and theoretical data on the $A^2\Pi$ state of MXe molecules. Methods, bond length (in atomic units), and dissociation energies (in cm^{-1}). PW: present work.

Molecule	Reference	Method	R_e	D_e
LiXe	41	Expt.	5.99	1650
	19	MRCI ($A^2\Pi_{1/2}$)	5.40	1461
	19	MRCI ($A^2\Pi_{3/2}$)	5.44	1332
	PW	CCSD(T)	5.32	1730
NaXe	42	Expt.	6.25	1130
	14	Expt. ($A^2\Pi_{1/2}$)	6.05	1215
	14	Expt. ($A^2\Pi_{3/2}$)	6.08	1120
	PW	CCSD(T)	6.11	1094
KXe	PW	CCSD(T)	6.94	740

state (see Table I) is not observed here and both calculations give almost the same R_e. However, the well depth D_e differs by 5%. Both CCSD(T) calculations were performed with much larger basis set than the MRCI calculation of Park *et al.*[19] and produces shorter and deeper potential well, though the latter calculation was apparently not corrected for BSSE. For the $B^2\Sigma^+$ state, our CASPT2 calculation is relatively close to the CCSD(T) calculation of Kerkines and Mavridis,[17] as it can be observed in Figure 6. In the repulsive part, the CASPT2 curve is shifted by 50 cm^{-1} above the CCSD(T) curve. Regarding our model calculation, the long-range behavior is remarkably close to the CCSD(T), while more significant difference is observed around $R = 5$ a.u.

We first analyze the $A^2\Pi$ state of NaKr dimer for ^{84}Kr isotope. Its vibrational structure has been investigated experimentally in great detail[13] and offers an excellent benchmark for the accuracy of our calculation. Our calculation indicates 28 and 25 vibrational states for $\Omega = 1/2$ and $\Omega = 3/2$, respectively. The experiment probes the medium vibrational levels range, from $\nu = 7$ to $\nu = 14$. The energy difference $T(\nu, \nu')$ between two rotationless vibrational levels ν and ν' are, for example, $T(14, 7) = 205.6$ cm^{-1} and $T(13, 8) = 145.5$ cm^{-1} from our calculation, instead of 220.0 and 152.5, respectively, for the experiment. This suggests that the $A^2\Pi$ adiabatic well resulting from our calculation is not deep enough or too broad. The rotational constants $B(\nu)$ obtained as the difference between the two lowest rotational levels associated with a given vibrational level ν are, for example, $B(7) = 0.0727$ cm^{-1}, $B(10) = 0.0616$ cm^{-1}, and $B(13) = 0.0503$ cm^{-1}, as compared to $B(7) = 0.0737$ cm^{-1}, $B(10) = 0.0626$ cm^{-1}, and $B(13) = 0.0513$ cm^{-1} experimentally. The effective rotational constant deduced from experiment is thus systematically larger than our $B(\nu)$ by 1%–2%. Considering the R^{-2} dependence of the centrifugal energy, the underestimation of $B(\nu)$ suggests that the actual potential well is more attractive at short distance. In other words, the inner classical turning point should be shifted toward shorter R or the potential well deepened with respect to our calculation.

The adiabatic $B^2\Sigma^+$ state obtained by means of CASPT2 calculations is compared with the potential extracted from collisional experiment[43] for NaKr in Figure 6. As it can be observed, the extracted curve is far above our results. A more correlated method will definitely produce a curve below the

CASPT2, as it is the case for LiKr, and the curve extracted from experiment is probably not reliable for $R < 9$ a.u. For larger distances, we used the model potential to obtain the $B^2\Sigma^+$ PEC. It is indeed in close agreement with CCSD(T) calculation in the case of LiKr, and certainly better than the CASPT2 calculation in the energy range of interest here. Our model calculation produces a potential well with $D_e = 59$ cm^{-1} at $R_e = 12.75$ a.u., i.e., 20 cm^{-1} below the CASPT2 results for NaKr. This depth is comparable to the value obtained for LiKr.

We turn now our analysis to the spin-orbit coupling for NaKr. Its effect can be observed on the transition energies $T_{A_\Omega X}(\nu, 0)$ from the vibrational state $\nu' = 0$ of the electronic ground state to the vibrational state ν of the A_Ω state. After removing the small difference between experimental and calculated atomic transition energies, we obtain $T_{A_{\frac{3}{2}}X}(14, 0) = 16\,958.8$, $T_{A_{\frac{1}{2}}X}(14, 0) = 16\,942.4$, $T_{A_{\frac{3}{2}}X}(7, 0) = 16\,756.6$, and $T_{A_{\frac{1}{2}}X}(7, 0) = 16\,733.1$ cm^{-1}. The difference with the corresponding experimental values are $+1.2$, $+5.2$, $+8.4$, and $+17.6$ cm^{-1}, respectively. The calculated values are systematically larger than the experimental ones. It is worth noting here that the transition energy depends on the actual energy of the lowest vibrational state $\nu' = 0$ of the electronic ground state with respect to its dissociation limit. Using a deeper vibrational ground state, as suggested by experimental results, would enlarge the transition energy and thus the difference between experiment and theory. An estimate of the computational accuracy can be obtained from the difference between the Ω-averaged experimental transition energy from a given ν and the corresponding spin-free computed values. The difference is of the order of 4%, suggesting that the real $A^2\Pi$ potential well is comparably deeper than our calculated PEC.

The near degeneracy of the $A_{\frac{3}{2}}$ $\nu = 13$ and $A_{\frac{1}{2}}$ $\nu = 14$ states observed experimentally is very well reproduced by our calculation. However, the variation of the SO splitting $\Delta_{SO}(\nu)$ with respect to ν is underestimated. For example, we obtain $\Delta_{SO}(7) = 23.5$ and $\Delta_{SO}(14) = 16.5$ cm^{-1} instead of 32.6 and 20.4 cm^{-1} experimentally. In this range of ν values, the upper $B^2\Sigma^+$ state is well separated from the $A^2\Pi$ states and has thus little influence on the vibrational levels. The SO effect is dominated by the coefficient $a(R)$ rather than $b(R)$. It is thus likely that $a(R)$ is actually larger than predicted by our RASSCF-AMFI calculation. Other contributions to this discrepancy may arise also from differences in the shape of the adiabatic $A^2\Pi$ curve, which would change the vibrational wave functions and energies. For example, a shift of the PEC toward shorter R by approximately 1%, consistent with the difference observed for the rotational constant, would improve the comparison.

We turn now our attention to the NaXe dimer. We focus here on the ^{129}Xe isotope for which we found 33 and 29 vibrational levels for $\Omega = \frac{1}{2}$ and $\Omega = \frac{3}{2}$, respectively. The vibrational structure of the electronic $A^2\Pi$ states was also investigated experimentally[14] for the vibrational levels $\nu = 10$–16. Looking first at the average rotational constant $B(\nu)$, we observe that our calculation is in excess with respect to experimental values by 1% for $B(10)$ and up to 4% for $B(16)$. This

difference is striking, because it suggests that the positions of the classical inner turning points of our calculated PEC are too short, while it is expected that any improvement of the calculation would produce a more compact PEC, with slightly shorter inner turning point positions. Moreover, this difference is not consistent with the difference observed for the NaKr molecule, for which the calculation produces a smaller $B(\nu)$ than observed experimentally.

To calculate the transition energies $T_{A_\Omega X}(\nu, 0)$ as defined above, we used the CCSD(T) PEC for the $X^2\Sigma^+$ and $A^2\Pi$ states and we simply used the CASPT2 calculation of the $B^2\Sigma^+$ state. In the range $\nu = 10$–16 recorded experimentally, the vibrational energy is at least 135 cm^{-1} below the asymptotic limit, and the effect of the coupling between A and B states has only a minor influence. Since both states, A and X, were obtained from CCSD(T) calculations, we expect the calculated transition energies $T_{A_\Omega X}(\nu, 0)$ to be reliable. After correction for the small difference between experimental and calculated atomic transition energies, we obtain $T_{A_{\frac{3}{2}}X}(16, 0) = 16\,923.5$, $T_{A_{\frac{1}{2}}X}(16, 0) = 16\,895.7$, $T_{A_{\frac{3}{2}}X}(10, 0) = 16\,711.2$, and $T_{A_{\frac{1}{2}}X}(10, 0) = 16\,669.9$ cm^{-1}. Our calculated transition energies exceed the corresponding experimental values. The differences are 22.0, 39.0, 31.5, and 58.5 cm^{-1}, respectively. They are significantly larger than the differences observed for NaKr. As noted in Sec. III, there is also a large difference of 22 cm^{-1} between the lowest vibrational levels of our calculated ground state and the fit deduced from experiment. Using this fitted curve instead of the calculated, one would increase the observed difference in the transition energies $T_{A_\Omega X}(\nu, 0)$. There is no obvious explanation why our calculation should be significantly less accurate for Xe than for Kr. We notice that the difference is of the order of one vibrational level spacing. Such a discrepancy might be explained by a shift in the assignment of the vibrational levels.

Regarding the variation of the spin-orbit coupling with ν, we obtain $\Delta_{SO}(10) = 41.3$ and $\Delta_{SO}(16) = 27.8$ cm^{-1}. It is larger than the corresponding values for NaKr, but significantly smaller than the values deduced from experiment, 68.3 and 44.8, respectively. A shift by 1 vibrational level would change the latter values by 4 cm^{-1} typically. The remaining part reflects the limitation of the SO coupling at the RASSCF-AMFI level on one hand, and of the adiabatic PEC at the CCSD(T) level on the other hand.

The analysis of the long-range part of the PEC is not easy because the binding energy becomes rapidly very small and its numerical accuracy deteriorates rapidly as R increases. At $R = 20$ a.u. the binding energies of the $A^2\Pi$ states are of the order of a few cm^{-1} and we expect the numerical accuracy of the CCSD(T) calculation to be of the order of 1% of this energy. Like for the ground state, we define $Q(R) = R^6 V(R)$, where V(R) is the binding energy of the dimer. The values $Q(20)$ are compared to the result of the expansion obtained with the coefficients determined by Mitroy and Zhang[35] in Table VI. For Li and Na, we observe a fair agreement of the order of a few percent with the values deduced from expansion coefficient. The agreement is not as good for K, for which the difference is of the order of 20% for both Kr and Xe.

TABLE VI. Asymptotic values of $Q(R) = R^6 V(R)$ and $Q^*(R) = C_6 + C_8/R^2 + C_{10}/R^4$ for MRG pairs at $R = 20$ a.u., for the $A^2\Pi$ state. The coefficients C_n are taken from Ref. 35. All values are given in atomic units.

Dimer	$Q(20)$	$Q^*(20)$	C_6	$\frac{C_8}{R^2} + \frac{C_{10}}{R^4}$
LiKr	340	349	330	19
LiXe	544	563	524	39
NaKr	521	546	512	34
NaXe	841	883	817	66
KKr	646	760	706	54
KXe	1052	1220	1123	97

VI. CONCLUSION

The present determination of the PEC of alkali-rare gas dimers is based on all-electron, highly correlated, size consistent and BSSE corrected method. It includes scalar relativistic corrections and large basis sets were used in an attempt to obtain accurate reference data. The accuracy of the results is estimated by comparison with the most accurate experimental results obtained from vibrational spectroscopy analysis.

For NaKr, the analysis of the rotational constant suggests that the calculated minimum energy positions R_e are too long by 1% for both $X^2\Sigma^+$ and $A^2\Pi$ states. The analysis of the AX transition energies indicates that the well depth D_e of the $A^2\Pi$ state is underestimated by an amount of 4% at least.

The comparison with the experimental results for NaXe is more puzzling. Our calculation predicts a larger rotational constant for the $A^2\Pi$ state, though the equilibrium distance R_e is very close to the value deduced from experiment. This result is unexpected for such kind of calculations, and it might actually be due to an incorrect assignment of the vibrational levels from the measured transition energies.

The internal consistency of the method suggests that R_e are systematically in excess by approximately 1% for all alkali-RG pairs investigated here for both $X^2\Sigma^+$ and $A^2\Pi$ states. We estimate the systematic error regarding D_e to be of the order of 4%–10%. The large contribution of triple excitations to the correlation energy (up to 35% of D_e for KXe in the $X^2\Sigma^+$ state and up to 15% in the $A^2\Pi$ state) suggests that the exact triple and quadruple excitations are actually important and might lower D_e by such an amount.

An important feature of the alkali-RG dimers is the so called heavy element effect, which enhances the atomic spin-orbit splitting between the $\Omega = \frac{1}{2}$ and $\Omega = \frac{3}{2}$ states. For the intermediate vibrational states accessible to experiment, the SO coupling is dominated by $a(R)$. The coefficient varies significantly with the interatomic distance because of the hybridization of the valence orbital, which acquires some rare gas p character as the molecule forms. Our calculation shows clearly that the heavy element effects becomes less and less significant as the atomic number of the alkali increase. Our calculation is in close agreement with previous calculation of $a(R)$ for Li-RG dimers.[18,19] However, the comparison with experimental results obtained for NaKr and NaXe suggests that the calculated coefficients $a(R)$ are too small. The upper part of the vibrational spectrum is dominated by the coefficient $b(R)$ and to some extent by the non-adiabatic coupling between $A^2\Pi$ and $B^2\Sigma^+$ states. There is no experimental data available for the highly excited vibrational states of the dimers investigated here and our knowledge of the adiabatic $B^2\Sigma^+$ state is not as accurate as the $X^2\Sigma^+$ and $A^2\Pi$ states. Nevertheless, it is important to keep in mind that the vibrational properties of the A and B $\Omega = \frac{1}{2}$ states is controlled by the coefficient $b(R)$, which behaves in an opposite way as $a(R)$ with the interatomic distance R. For LiKr and LiXe, it is remarkable that this coefficient vanishes at a distance comparable to the adiabatic $A^2\Pi$ and $B^2\Sigma^+$ curve crossing, making the non-adiabatic coupling potentially important in the determination of the vibrational energy levels.

Anticipating future developments, the present analysis will be used to develop accurate model potentials including spin-orbit effects on firm grounds. In particular, the combination of our work with experimental results can be used to extract more accurate PEC for NaRG in a first step, and then extending it to the other alkali, for which experimental results are not available, by means of scaling laws. These PEC could be used to build model potentials including SO effects to study collisions between excited alkali and heavy rare gas. They will be used to investigate more complex situations like the relaxation dynamics of alkali atoms trapped at the surface of Kr and Xe clusters. Such kind of non-adiabatic dynamics are very sensitive to the details of the PEC, in particular curve crossings, which allows the system to switch from an adiabatic electronic state to another one.

[1] L. C. Balling and J. J. Wright, J. Chem. Phys. **79**, 2941 (1983).

[2] J. A. Boatz and M. E. Fajardo, J. Chem. Phys. **101**, 3472 (1994).

[3] M. Ryan, M. Collier, P. de Pujo, C. Crépin, and J. G. McCaffrey, J. Phys. Chem. A **114**, 3011 (2010).

[4] M. Groß and F. Spiegelmann, J. Chem. Phys. **108**, 4148 (1998).

[5] E. Jacquet, D. Zanuttini, J. Douady, E. Giglio, and B. Gervais, J. Chem. Phys. **135**, 174503 (2011).

[6] C. J. Lee, M. D. Havey, and R. P. Meyer, Phys. Rev. A **43**, 77 (1991).

[7] C. J. Lee and M. D. Havey, Phys. Rev. A **43**, 6066 (1991).

[8] R. Brühl and D. Zimmermann, J. Chem. Phys. **114**, 3035 (2001); **115**, 7892 (2001).

[9] W. P. Lapatovich, R. Ahmad-Bitar, P. E. Moskowitz, I. Renhorn, R. A. Gottscho, and D. E. Pritchard, J. Chem. Phys. **73**, 5419 (1980).

[10] R. A. Gottscho, R. Ahmad-Bitar, W. P. Lapatovich, I. Renhorn, and D. E. Pritchard, J. Chem. Phys. **75**, 2546 (1981).

[11] D. Schwarzhans and D. Zimmermann, Eur. Phys. J. **22**, 193 (2003) and reference therein.

[12] E. Zanger, V. Schmatloch, and D. Zimmermann, J. Chem. Phys. **88**, 5396 (1988).

[13] R. Bruhl, J. Kapetanakis, and D. Zimmermann, J. Chem. Phys. **94**, 5865 (1991).

[14] P. Baumann, D. Zimmermann, and R. Bruhl, J. Mol. Spectrosc. **155**, 277 (1992).

[15] F. Bokelmann and D. Zimmermann, J. Chem. Phys. **104**, 923 (1996).

[16] I. S. K. Kerkines and A. Mavridis, J. Phys. Chem. A **104**, 408 (2000); **105**, 1983 (2001).

[17] I. S. K. Kerkines and A. Mavridis, J. Chem. Phys. **116**, 9305 (2002).

[18] K. Sohlberg and D. R. Yarkony, J. Chem. Phys. **107**, 7690 (1997).

[19] S. J. Park, Y. S. Lee, and G.-H. Jeung, Chem. Phys. Lett. **325**, 678 (2000).

[20]F. Aquilante, L. De Vico, N. Ferre, G. Ghigo, P.-A. Malmqvist, P. Neograly, T. B. Pedersen, M. Pitonak, M. Reiher, B. O. Roos, L. Serrano-Andrés, M. Urban, V. Veryazov, and R. Lindh, J. Comput. Chem. **31**, 224 (2010).

[21]D. Zanuttini, E. Jacquet, E. Giglio, J. Douady, and B. Gervais, J. Chem. Phys. **131**, 214104 (2009).

[22]E. Czuchaj, F. Rebentrost, H. Stoll, and H. Preuss, Chem. Phys. **136**, 79 (1989).

[23]M. B. El Hadj Rouma, H. Berriche, Z. B. Lakhdar, and F. Spiegelmann, J. Chem. Phys. **116**, 1839 (2002) and reference therein.

[24]T. Nakajima and K. Hirao, Chem. Rev. **112**, 385 (2012).

[25]M. Reiher, WIREs: Comput. Mol. Sci. **2**, 139 (2012).

[26]B. O. Roos, V. Veryazov, and P.-O. Widmark, Theor. Chem. Acc. **111**, 345 (2004).

[27]B. O. Roos, R. Lindh, P.-A. Malmqvist, V. Veryazov, and P.-O. Widmark, J. Phys. Chem. A **108**, 2851 (2004).

[28]S. F. Boys and F. Bernardi, Mol. Phys. **19**, 553 (1970).

[29]C. E. Moore, *Atomic Energy Levels*, NBS Circular No. 467 (U.S. Government Printing Office, Washington, DC, 1958).

[30]B. A. Hess, C. M. Marian, U. Wahlgren, and O. Gropen, Chem. Phys. Lett. **251**, 365 (1996).

[31]J. Lozeille, E. Winata, P. Soldán, E. P. F. Lee, L. A. Viehland, and T. G. Wright, Phys. Chem. Chem. Phys. **4**, 3601 (2002).

[32]L. A. Viehland, J. Lozeille, P. Soldán, E. P. F. Lee, and T. G. Wright, J. Chem. Phys. **119**, 3729 (2003).

[33]L. A. Viehland, J. Lozeille, P. Soldán, E. P. F. Lee, and T. G. Wright, J. Chem. Phys. **121**, 341 (2004).

[34]See supplementary material at http://dx.doi.org/10.1063/1.4773019 for computed values of Figs. 1–4, 6, and 7.

[35]J. Mitroy and J.-Y. Zhang, Phys. Rev. A **75**, 032706 (2007).

[36]J. M. Standard and P. R. Certain, J. Chem. Phys. **83**, 3002 (1985).

[37]K. Sohlberg and D. R. Yarkony, J. Phys. Chem. A **101**, 3166 (1997).

[38]U. Buck and H. Pauly, Z. Phys. **208**, 390 (1968).

[39]R. Duren, G. P. Raabe, and C. Schlier, Z. Phys. **214**, 410 (1968).

[40]D. J. Auerbach, J. Chem. Phys. **60**, 4116 (1974).

[41]R. Scheps, C. Ottinger, G. York, and A. Gallagher, J. Chem. Phys. **63**, 2581 (1975).

[42]G. York, R. Scheps, and A. Gallagher, J. Chem. Phys. **63**, 1052 (1975).

[43]J. Grosser, O. Hoffmann, S. Klose, and F. Rebentrost, Europhys. Lett. **39**, 147 (1997).